TWELFTH EUROPEAN ROTORCRAFT FORUM

Paper No. 47

SOME SOVIET AND WESTERN SIMPLIFIED HELICOPTER PERFORMANCE PREDICTION METHODS IN COMPARISON WITH TESTS

W. Z. Stepniewski
International Technical Associates, Ltd.
Drexel Hill, Pa. USA

W. R. Burrowbridge
Aerospace Engineer, US Army
Charlottesville, Va. USA

September 22 – 25, 1986

Garmisch-Partenkirchen
Federal Republic of Germany

Deutsche Gesellschaft für Luft- und Raumfahrt e. V. (DGLR)
Godesberger Allee 70, D-5300 Bonn 2, F.R.G.

ABSTRACT

Since Western simplified helicopter performance predictions were discussed by Gessow in his 1985 Nikolsky Lecture[1], attention has been focused on Soviet procedures as exemplified in Vil'dgrube's book entitled *Helicopters*[2]. Using the simplified approaches from that book, the following aspects of hover OGE were examined for single-rotor and coaxial configurations: (a) determination of basic characteristics of isolated rotors, (b) download calculations for helicopters, and (c) predictions of helicopter *SHP required*. *Horizontal* flight aspects were examined by determining the SHP required by single-rotor helicopters. Predicted figures for several Western helicopters and NACA coaxial rotors were compared with full-scale ground and/or flight test results, generally showing good to very good agreement. In addition, some basic aspects of the flat-wake concept are also briefly discussed.

LIST OF SYMBOLS

A	total rotor disc area in sq.ft
b	number of blades
c	*chord in ft*
c_d	section drag coefficient
c_l	section lift coefficient
C_P	power coefficient
C_Q	rotor torque coefficient
C_T	rotor thrust coefficient
C_W	gross-weight coefficient
d_z	distance between rotor axes in ft
D_v	vertical drag in lb
f	equivalent flat-plate area in sq.ft
$\hat{f} = f/W$	equivalent flat-plate area per pound of gross weight in sq.ft/lb
FM	figure of merit
$\bar{h}_{rr} = h_{rr}/R$	relative elevation of the rear rotor
I or I_0	induction coefficient, excluding tip losses
k_{ov}	induced power coefficient for overlapping rotors
$k_{\mu r}$	taper influence coefficient (profile power)
k_T	taper influence coefficient (thrust)
$\bar{l}_{tr}$	relative distance between main and tail-rotor axes
$\bar{l}_w = l_w/R$	relative wing span
M	Mach number
ov	overlap
r	distance from rotor axis in ft
$\bar{r} = r/R$	blade station
R	rotor radius in ft
Re	Reynolds number
RP	rotor power in hp or ft-lb/sec
S	surface area in sq.ft
$\bar{S}_w = S_w/\pi R^2$	*relative wing area*
T	thrust in lb
$\bar{T} = T/W$	thrust to gross-weight ratio
v	induced velocity in fps
V	*flight velocity in knots or fps*
w	disc loading in psf
$W = GW$	gross weight in lb
y_t	vertical rotor separation in ft
α	angle of attack in deg. or rad
α_ϵ	thrust vector inclination in deg or rad
α_*	relative distance between the tip vortex filaments
$\bar{\Gamma} = \Gamma/R^2\Omega$	relative circulation
Δ	increment
$\Delta\bar{T}$	relative download
η_{oa}	overall transmission efficiency
η_*	blade taper ratio
θ	pitch angle in deg. or rad
$\mu \approx \bar{V}$	advance ratio
ρ	*air density in slugs/cu.ft*
σ	rotor solidity
σ_ρ	relative air density
ϕ	induced inflow angle in deg or rad
χ	tip-loss factor
ΩR	rotor tip speed in fps

Subscripts

co	coaxial	*rr*	rear rotor
cool	cooling losses	$\bar{r}$	blade station
f, or *fu*	fuselage	*sr*	single rotor
h	hover	*tan*	*tandem*
he	horizontal empennage	*tr*	tail rotor
hz	horizontal	*tw*	twist
ind	induced	*tx*	transmission
oa	overall	*w*	wing
pa	parasite	*2s*	two single rotors
pr	profile	Σ	total
req	required	2, 4.5, etc.	blade station @ $\bar{r}$ = 0.2, 0.45, etc

Superscripts

$\bar{}$	relative, with respect to R, πR^2, and ΩR, etc.
$\sim$	ratio

SOME SOVIET AND WESTERN SIMPLIFIED HELICOPTER PERFORMANCE PREDICTION METHODS IN COMPARISON WITH TESTS

by

W. Z. Stepniewski
International Technical Associates, Ltd.
Drexel Hill, Pa, USA

W. R. Burrowbridge
Aerospace Engineer, US Army
Charlottesville, Va, USA

1. Introduction

In the domain of predicting aerodynamic characteristics of isolated rotors and performance of complete rotary-wing aircraft, one should note that in the West there is a definite tendency toward larger and larger computational programs based on more and more complex conceptual models. However, in parallel with this drive toward perfection through sophistication and complexity, there seems to exist a genuine need for some approximate, but simple, solutions to the problem of quantitative evaluation of various phenomena of rotary-wing aerodynamics. This is especially true with respect to performance predictions where simplified methods should obviously be quite useful in practical engineering in such applications as concept formulation and preliminary design of rotorcraft.

As far as Western rotary-wing technology is concerned, the whole aspect of simple approaches was very ably discussed by Gessow in his 1985 Nikolsky Honorary Lecture[1]. There, he indicated and supported his statement by numerous examples that many of the approaches taken during the early years of helicopter development are still capable of predicting aerodynamic characteristics of isolated single- and multi-rotor configurations with good, and often better, accuracy than those obtained through sophisticated computer programs. This was true in spite of the fact that those early approaches were usually based on simple concepts of the combined blade-element and momentary theories, or uncomplicated vortex systems.

It is obviously of interest to know whether in the other important school of rotary-wing technology – namely, in the Soviet Union – there is a trend, or at least a discussion, related to the use of simple approximate methods in solving some practical engineering problems of rotary-wing aerodynamics and especially, performance prediction of helicopters.

In this respect, Vil'dgrube's book entitled *Helicopters – Calculation of Integral Aerodynamic Characteristics and Flight-Mechanics Data*[2] may be cited as an example of an effort in that direction. This book may also be considered as a companion text to *Theory of the Lifting Airscrew*[3] (coauthored by Vil'dgrube), from whose sophisticated contents the author of Ref. 2 worked out a series of formulas and graphs which would be helpful, not only to perform the aerodynamic calculations, but also to expeditiously select the configuration of the lifting-rotor blade and parameters of the helicopter.

It should be noted at this point that in Refs. 2 and 3 the interpretation of the physical aspects of aerodynamic phenomena encountered by the rotor, as well as the resulting computational procedures, were almost entirely based on the vortex theory (called the Joukowsky theory in both books). However, in Ref. 2, the scope of the conceptual models based on this principle is much narrower.

In Ref. 3, *Theory of the Lifting Airscrew*, the blades were modeled by both lifting line and vorticity surfaces, and various wake types ranging from noncontracting cylindrical wakes in axial translation to completely free wakes in both axial translation and in flights with horizontal components were examined.

By contrast, In Ref. 2, the blades are exclusively modeled by single lifting lines, while rotor wakes are assumed to be of cylindrical shapes in hover and vertical translation, and are considered to be flat in forward flight. Examination of the shapes of spanwise circulation distribution combined with noncontracting cylindrical wake concepts became one of the principal tools in developing practical formulas for performance predictions in hover and vertical translation. Forward flight phenomena are chiefly interpreted with the help of the flat-wake concept, although a strict applicability of that approach is limited to the following range of advanced ratios:

$$1.63\sqrt{C_T} \leqslant \mu \approx \overline{V} \leqslant 0.25.$$

When Vil'dgrube's book was reviewed by the authors of this paper, it became clear that the Soviet text contained many potentially useful simple approximate methods and procedures for determining aerodynamic characteristics of isolated single and multirotor configurations and performance predictions of complete conventional helicopters of single-rotor, coaxial, and tandem configurations. It also contained such interesting simplifications as performance predictions of winged and compound helicopters, as well as rotor optimization in hover and forward flight. The question, however, is whether these approaches are consistently accurate enough to make them suitable for practical engineering applications.

In order to ascertain the answer to this question, it was postulated that some of the short-cut approaches taken by Vil'dgrube would be selected and applied to the calculations of aerodynamic characteristics of Western isolated rotors and performance predictions of complete helicopters. The results would then be compared with data from actual flight tests or experimental data preferably obtained from full-scale tower or wind-tunnel tests.

The following cases are presented as examples of such comparisons.

- Hover OGE
  a. Aerodynamic characteristics of single isolated rotors
  b. Aerodynamic characteristics of coaxial isolated rotors
  c. Helicopter download
  d. Helicopter engine power required
- Engine Power Required in Horizontal Flight
  a. Formulation of the problem
  b. Flat-wake concept
  c; Aerodynamic interaction of twin-rotor configurations
  d. Single-rotor helicopter

Obviously, one would find that some of the simplified procedures of Ref. 2 are, in principle, quite similar to those used in the West and have been described in numerous reports and such textbooks on rotary-wing aerodynamics as, for instance, Refs. 4 and 5. However, there is enough difference in the philosophy of presentation and formulation of actual procedures to merit examination of Vil'dgrube's approaches in their original forms. Therefore, in order to facilitate the Western reader in following this paper, all formulas taken from Ref. 2 and presented here have been converted using Western symbols and coefficients and U.S. units of measure. The procedures are described in sufficient detail to enable one to perform his/her own calculations.

2. Hover

2.1 Aerodynamic Characteristics of Single Isolated Rotors in Hover OGE

2.1.1 General

Ways of calculating the characteristics of single isolated rotors in hover OGE are presented by first using the four-section, and then the single (representative) blade section computational approaches from Ref. 2. Both approaches are applied to the YUH-61A rotor, representing rotors with rectangular blades. For the case of rotors with tapered blades, a single rotor from the NACA coaxial configuration is examined, using the single-section approach only.

2.1.2 Outline of Procedure for Four-Section Approach

The procedures outlined here for the case of four-blade sections can obviously be extended to a larger number of blade stations once the basic principle of that approach is understood.

The four-section procedure presented here adheres to the outline given in Section 1.1 of Ref. 2, where $\bar{r} = 0.2, 0.45, 0.7$, and 0.95 were selected as representative blade stations.

A relationship between the blade-section lift coefficient ($c_{l_{\bar{r}}}$) and the blade-section pitch angle ($\theta_{\bar{r}}$) was established and then presented in graphical form.

The steps required for the determination of the $c_l = f(\theta_{\bar{r}})$ relationship can be summarized as follows: several local c_l values (say, 0, 0.2, ...1.0) are assumed for each of the representative sections, and the corresponding angle-of-attack values for the local airfoil sections are determined from the $c_l = f(\alpha)$ graphs at proper Reynolds and Mach number values. Next, the corresponding relative circulation ($\bar{\Gamma}_{\bar{r}}$) is computed for the assumed sectional c_l values:

$$\bar{\Gamma}_r = \tfrac{1}{2} c_{l_{\bar{r}}} \bar{c}_{\bar{r}} \bar{r} \tag{1}$$

where $\bar{c}_r$ is the relative blade chord ($\bar{c}_{\bar{r}} = c_r/R$) at station $\bar{r}$.

Knowing the local circulation, the corresponding local induced velocity in nondimensional form ($\bar{v}_{\bar{r}}$) is computed:

$$\bar{v}_{\bar{r}} = \tfrac{1}{2}\sqrt{b\bar{\Gamma}_{\bar{r}}/\pi} \tag{2}$$

where b is the number of blades. The induced inflow angle (ϕ_r) is then obtained:

$$\phi_{\bar{r}} = \arctan \bar{v}_{\bar{r}}/\bar{r}. \tag{3}$$

The sum of the local inflow angle and the blade section angle of attack gives the local pitch angle ($\theta_{\bar{r}}$) required for obtaining the assumed local blade-lift coefficient value. From this data, a graph expressing the $c_{l_{\bar{r}}} = f(\theta_{\bar{r}})$ relationship can now be plotted (for example, see Fig. 1).

The procedure required for computing $C_T = f(C_Q)$ are quite simple: Several values of the collective pitch angle θ_0, defined as $\theta_0 \equiv \theta_{.7}$, are assumed. Knowing the built-in blade twist ($\theta_{tw} = f(\bar{r})$) and thus, the twist increment ($\Delta\theta^\circ_{\bar{r}}$) at each of the representative blade sections, the local blade pitch angle corresponding to the assumed blade collective pitch values can be determined as

$$\theta_{\bar{r}} = \theta_0 - \theta_{tw}(\bar{r}). \tag{4}$$

Then, from the previously prepared $c_l = f(\theta_{\bar{r}})$ graph, the corresponding values of c_{l_2}, $c_{l_{4.5}}$, etc., can be read. This, in turn would permit one to find the c_d values associated with the previously obtained c_l's from the $c_d = f(c_l)$ relationship for the local airfoil sections at the proper Mach and Reynolds numbers.

The C_T values can now be determined (either graphically or numerically) from the following:

$$C_T = \tfrac{1}{2}\chi(b/\pi)\int_{\bar{r}_0}^{1.0} c_l \bar{c}_{\bar{r}}^{\,2}\, d\bar{r}. \tag{5}$$

where χ is the tip-loss factor whose value is usually assumed in Ref. 2 as 0.94. The rotor thrust coefficients can be computed for each assumed collective pitch angle. However, should the so-obtained C_T value be so high that

$$\sqrt{C_T}/b > 0.025, \tag{6}$$

a new tip-loss factor value must be estimated from Fig. 2 (Fig. 1.2^2) as follows.

Compute $\bar{\alpha}_*$, which represents the relative distance between the tip vortex filaments, as

$$\bar{\alpha}_* = 2\pi\bar{v}/b, \tag{7}$$

where $\bar{v}$ is the relative induced velocity averaged over the rotor disc, and may be assumed as approximately equal to the ideal induced velocity, including the tip-loss factor

$$\bar{v} = 0.707\sqrt{C_T/\chi} \tag{8}$$

or $\bar{v}$ may be approximated by $\bar{v}_{.7}$; i.e., induced velocity at $\bar{r} = 0.7$.

Read the new tip-loss factor value from Fig. 2.

Since two different shapes of radial circulation distribution are assumed in Fig. 2, the character of the actual circulation distribution along the blades must be established in order to read a correct figure value (say, by plotting $\bar{\Gamma}_{\bar{r}}$ vs. $\bar{r}$).

Once the correct levels of the tip-loss factor (χ) are verified, further computations of $C_{Q_{ind}}$ can be continued by enumerating the values (numerically or graphically) of the following integral:

$$C_{Q_{ind}} = (b/\pi)\int_{\bar{r}_0}^{1} \bar{\Gamma}_{\bar{r}}\bar{r}\bar{v}_{\bar{r}}\, d\bar{r} \tag{9}$$

where the $\bar{v}_{\bar{r}}$ values are computed from Eq. (2).

The $C_{Q_{pr}}$ values are estimated (again, graphically or numerically) from the following integral:

$$C_{Q_{pr}} = (b/2\pi) \int_0^1 c_{d_{\bar{r}}} \bar{c}_{\bar{r}}^3 \, d\bar{r}, \tag{10}$$

where $c_{d_{\bar{r}}}$ values obviously correspond to $c_{l_{\bar{r}}}$ at proper Mach and Reynolds numbers.

Finally, $C_Q = C_p$ is calculated as

$$C_Q = C_{Q_{ind}} + C_{Q_{pr}}. \tag{11}$$

Now, the $C_T = f(C_Q)$ or $FM = f(C_T/\sigma)$ relationships can be compared with experimental figures.

2.1.3 Outline of Procedures for Single-Section Approach

Basic Approach. The single-section approaches of Ref. 2 represent one of the simplest ways of approximately determining aerodynamic characteristics of isolated rotors (incorporting either rectangular or tapered blades) of single and twin configurations in hover OGE. In both cases, rotor characteristics are derived from aerodynamic events occurring at the representative blade section, assumed in Ref. 2 to be located at $\bar{r} = 0.7$. The influence of these events, occurring at a single section, on the behavior of the whole rotor are interpreted with the aid of auxiliary graphs reflecting the significance of blade geometry; i.e., its planform and built-in twist.

The influence of the above two parameters on the rotor induced power coefficient I_0 – reflecting the influence of the nonuniformity of the downwash only on the ratio of actual induced power to the ideal power, but excluding tip losses – can be determined from Fig. 3 (originally Fig. 1.14[2]). The definition of the taper ratio is also given at the top of this figure.

The influence of the blade taper on the thrust coefficient (C_T) and profile torque coefficient ($C_{Q_{pr}}$) values can be interpreted with the help of the respective k_T and k_{pr} coefficients shown in Fig. 4 (based on values given in Ref. 2, pp 18 and 19).

Tapered Blades. Consecutive steps leading to the establishment of the C_T vs. C_Q relationship for rotors incorporating tapered blades begin with the assumption of several values of the average blade-lift coefficient (c_{l_0}), considered to be of the same value as c_{l_7}. Then, the c_d values corresponding to these c_{l_0}'s are determined, with due consideration of the Reynolds and Mach number values at $\bar{r} = 0.7$. Now, the rotor torque coefficient due to the profile power can be computed as

$$C_{Q_{pr}} = (1/8) k_{pr} c_{d_0} \sigma_7, \tag{12}$$

where the symbol σ_7 signifies that rotor solidity is based on the blade chord at $\bar{r} = 0.7$, and the k_{pr} coefficient accounts for the taper influence.

Next, the thrust coefficient C_T is determined as

$$C_T = 0.1563 k_T \sigma_7 c_{l_0}, \tag{13}$$

where the 0.1563 coefficient incorporates the tip loss factor of $\chi = 0.94$, and the k_T coefficient reflects taper influence.

Upon determining the induction factor I_0 due to the downwash nonuniformity depicted in Fig. 3, the *rotor torque coefficient* related to the induced power can be calculated as

$$C_{Q_{ind}} = 0.79 I_0 \, C_T{}^{1.5}. \tag{14}$$

Finally, the total rotor torque coefficient is computed as the sum of $C_{Q_{pr}}$ and $C_{Q_{ind}}$.

Rectangular Blades. For rectangular blades, the basic procedure is the same, with the exceptions that, obviously, k_T and $k_{pr} = 1.0$.

2.1.4 Comparison of Predictions with Test Results

Isolated Single Rotors. Using the four-section (2.1.2) and single-section (2.1.3) approaches, the C_T vs. C_P (C_Q) and *FM* vs. C_T/σ relationships were established for the following helicopter rotors: Boeing Vertol YUH-61A and CH-47D, Sikorsky S-76, and MBB BO-105 for which full-scale test results as well as all necessary inputs regarding blade geometry and airfoil characteristics at the required Reynolds and Mach numbers were available.

Figs. 5 and 6 are shown as typical examples where tower test[6] results are compared with the four- and single-section predictions for the YUH-61A rotor. Looking at these figures, one can see that in this case, the four-section method produced a very good agreement with the test data throughout the whole range of measured C_T and C_T/σ values.

The single-section approach appears to provide actual rotor performance equally well up to $C_T/\sigma \approx 0.07$ (Fig. 6). However, at $C_T/\sigma > 0.07$, predictions of the single-section procedure appear too optimistic. This, of course, should be anticipated, since the so-called representative station of $\bar{r} = 0.7$ does not adequately reflect aerodynamic events occurring in the tip region.

Results similar to those shown in Figs. 5 and 6 were also obtained for the three other investigated rotors. Absolute percentile deviations in the predicted figure-of-merit levels from those based on the full-scale obtained C_T and C_Q values are shown in Fig. 7. One can see from this figure that the trend discussed in conjunction with the YUH-61A rotor can be considered as the general one.

It appears, hence, that the four-section approach of Vil'dgrube is quite accurate in predicting performance of single rotors in hover OGE. Thus, it can be used with confidence, at least in the preliminary design and concept-formulation stages. The single-section approach of Ref. 2, in spite of its great simplicity, can also be of value in the above-mentioned tasks, at least for conventional helicopters, when C_T/σ is approximately lower than 0.06.

2.2 Isolated Coaxial Rotors in Hover OGE

2.2.1 General

A single expression for the rotor torque ($C_{Q_{co}}$) of the isolated coaxial configuration in vertical climb is given in Eq. (1.58) of Ref. 2. This expression can be transcribed for the case of hover OGE as follows:

$$C_{Q_{co}} = (C_{Q_{pr}})_{co} + 0.79 C_{T_{co}}{}^{3/2} I_0 \tag{15}$$

where the profile-drag torque coefficient $(C_{Q_{pr}})_{co}$ can be assumed as equal to twice the value of that for single rotors forming the coaxial configuration:

$$(C_{Q_{pr}})_{co} = 2C_{Q_{pr}}. \tag{16}$$

Assuming the more general case; i.e., that the rotor blades are tapered (for the definition of taper, η_*, see Fig. 3), the profile torque coefficient derived in the single-section approach for the single rotors of the coaxial configuration is given in Eq. (12) and thus, for the whole coaxial,

$$(C_{Q_{pr}})_{co} = \tfrac{1}{4}k_{pr}\sigma c_{d_0}. \tag{17}$$

As in the preceding section, k_{pr} is the taper ratio influence coefficient whose values are shown in Fig. 4, σ is the single rotor solidity ratio (defined as $\sigma = bc_7/\pi R = b\bar{c}_7/\pi$), and c_{d_0}, as always, is the profile drag coefficient at c_{l_0} and the corresponding Reynolds and Mach number values.

The induced torque coefficient is given by the second term in Eq. (15); i.e.,

$$(C_{Q_{ind}})_{co} = 0.79C_{T_{co}}{}^{3/2}I_0, \tag{18}$$

where $C_{T_{co}}$ is the rotor thrust coefficient based on the total thrust generated by the coaxial configuration, and I_0 is the induction coefficient whose value is established as for the single rotors (Fig. 3).

If the blades are tapered, the expression for $(C_{Q_{ind}})_{co}$ *will remain as given* by Eq. (18), except that the formula for the thrust coefficient will be as given by Eq. (13) and thus, will contain the taper ratio coefficient k_T:

$$C_{T_{co}} = 0.313k_T\sigma c_{l_0}, \tag{19}$$

where it should be remembered that σ is the solidity ratio for a single rotor.

2.2.2 Comparison of Predictions with Test Results

Using the single-section approach of Ref. 2 exclusively (discussed here in Sect. 2.1.3), C_T vs. C_Q and FM vs. C_T/σ relationships were computed for the following coaxial rotors for which *full-scale experimental* results and other necessary inputs were available: (a) NACA low-solidity coaxial rotor with tapered blades, (b) NACA high-solidity coaxial rotor with rectangular blades, and (c) Sikorsky ABC coaxial rotor. For the cases of (a) and (b), *full-scale measurements for the isolated coaxials were available*[7]. However, for the ABC rotor, the authors could not find any data regarding direct thrust and power measurements of the full-scale rotor; however, the C_P vs. C_W coefficients (based on engine power and aircraft flight weight – not rotor power and thrust) for the whole aircraft were available (Fig. 10). Following the procedure indicated in Ref. 8, the $C_{P_{co}}$ vs. $C_{T_{co}}$ relationship for the rotor alone was computed by assuming that the download amounts to 6 percent of the gross weight, and that power losses due to transmission and use of accessories are equal to 75 hp.

For example, the C_T vs. C_Q and FM vs. C_T/σ values computed for the NACA low-solidity coaxial with tapered blades are shown in Figs. 8 and 9 in comparison with the full-scale test results presented in Figs. 4 and 6 of Ref. 7.

A glance at Figs. 8 and 9 will indicate that, in general, very good to good agreement between the $C_{T_{co}}$ vs. $C_{Q_{co}}$ and FM vs. $C_{T_{co}}/\sigma_{co}$ relationships as calculated according to the procedures of Ref. 2, and those experimentally established through full-scale tests, can be registered.

Similar results were obtained for the NACA high-solidity coaxial with rectangular blades; whereas in the preceding case, experimental C_T and C_Q values were based on the direct thrust and rotor torque measurements. But, for the ABC helicopter, where characteristics of the isolated rotor were deduced from the flight test results, the predicted figures, on the average, overestimated the C_P values by about 3.5 percent (Fig. 10). Should, however, the assumed download and power losses (in estimating C_T and C_P's from the flight test data) be, say, 5 percent and 50 hp, respectively, instead of 6 percent and 70 hp, an almost perfect agreement with experimental results would be obtained.

After examining the three cases of hovering performance of full-scale coaxial rotors, one tends to conclude that the simple approach (based on a single-blade section) of Ref. 2 appears to be sufficiently accurate for preliminary performance estimates of coaxial rotors, assuming, as in the case of other rotors, that the rotor tip speeds are not so high as to generate considerable compressibility effects outboard of the 0.7 blade station.

2.3 Helicopter Download in Hover OGE

2.3.1 General

Elaborate procedures for determining helicopter download in hover OGE are described in Ref. 2. These procedures are based on various shapes of circulation distribution along the blades and vertical drag coefficient values of the helicopter body components exposed to the rotor slipstream (in many respects, these procedures are basically similar to those discussed by Keys in Vol. 2 of Ref. 5). But Vil'dgrube also gives very simple approximate formulas for estimating relative download ($\Delta\overline{T} = D_v/W$; i.e., vertical drag-to-gross-weight ratio) for helicopters of various configurations.

For single-rotor and coaxial helicopters with rotors having rectangular blades incorporating linear twist of $\theta_{tw} \approx 5^\circ$ to 7°, Eq. (2.15)[2] gives the following formulas for $\Delta\overline{T}$ values due to the wing ($\Delta\overline{T}_w$), fuselage ($\Delta\overline{T}_f$), and horizontal empennage ($\Delta\overline{T}_{he}$):

$$\begin{aligned} \Delta\overline{T}_w &\approx 0.375\overline{S}_w\overline{l}_w; \\ \Delta\overline{T}_f &\approx 0.238\overline{S}_f; \\ \Delta\overline{T}_{he} &\approx 1.38\overline{S}_{he} \end{aligned} \tag{20}$$

where $\overline{S}_w = S_w/\pi R^2$ is the relative wing area, $\overline{l}_w = l_w/R$ is the relative wing span, and $\overline{S}_{he} = S_{he}/\pi R^2$ is the relative horizontal empennage area.

For the tandem configuration, download on the fuselage would be

$$\Delta\overline{T}_{f_{tan}} \approx 0.11\overline{b}_f, \tag{21}$$

where $\overline{b}_f = b_f/R$ is the relative width of the fuselage.

2.3.2 Download Comparisons

The validity of Eqs. (20) and (21) was examined through direct and indirect comparisons.

Direct Comparison Rotor System Research Aircraft (RSRA). Material presented in Ref. 9 probably constitutes the only available full-scale experimental data regarding fuselage vertical drag in hover. The results of these measurements are presented on the right-side portion of Fig. 11 (based on Fig. 13 of Ref. 9), while the horizontal projection of the RSRA aircraft in the helicopter configuration is shown on the left-hand portion of this figure.

It can be seen from this projection that in hover only the fuselage is submerged in the rotor slipstream. Consequently, only the $\Delta\overline{T}_f$ expression in Eq. (20) was applied for the download estimation, leading to $(\Delta\overline{T}_f) \approx 0.0245$. Using this quantity, the total required rotor thrust was computed and plotted on the graph shown in the lower portion of the figure. It can be seen that in the 17,000-lb gross-weight area, there is complete agreement between predicted and measured rotor thrust values. At higher weights, the predicted rotor thrust values tend to become higher than the measured ones. However, an anomaly in the test data in Fig. 11 should be noted; namely, contrary to expectations, the fuselage drag *decreases* instead of increasing as the rotor disc loading increases.

Indirect Comparisons. Indirect download comparisons were made by computing relative downloads for single, coaxial, and tandem helicopters from Eqs. (20) and (21). The results were then compared with figures obtained through detailed analysis. All of the comparisons indicated a very good agreement with errors in $\overline{T}_h$ values remaining below the ±1 percent range (Fig. 12).

It appears, hence, that in spite of their simplicity, Eqs. (20) and (21) may be considered as useful tools for approximate predictions of download in hover OGE.

2.4 Helicopter Engine Power Required for Hover OGE

2.4.1 General

In principle, the already discussed approximate approaches for the determination of aerodynamic characteristics of isolated rotors and estimation of download should provide a way for obtaining most of the aerodynamic inputs needed for computation of helicopter engine power required in hover OGE. However, there are aerodynamic interactions (especially in the single-rotor configuration) which require additional attention. Thus, in order to give the reader a more complete picture of Vil'dgrube's approach to estimating engine power required through simplified procedures, the appropriate techniques of Ref. 2 are briefly reviewed for the single-rotor and coaxial configurations.

The computational procedure is based on determination of shaft horsepower in hover OGE $(\widetilde{SHP}_h)_{req}$ per pound of helicopter gross weight (W):

$$(\widetilde{SHP}_h)_{req} = (SHP_h)_{req}/W. \tag{22}$$

Once the values of $(\widetilde{SHP}_h)_{req}$ are determined, they can be converted (depending on the required mode of presentation) into total shaft horsepower required, or into a nondimensional form of the power coefficient $C_P = C_Q$.

To actually compute the shaft horsepower required, equations from Ref. 2 are rewritten in U.S. units and symbols as

$$(\widetilde{SHP}_h)_{req} = (\overline{T}_h/\eta_{oa})[0.00145(c_{d_0}/c_{l_0})\Omega R + 0.0290 I_0 \sqrt{(w/\sigma_\rho)\overline{T}_h}] \tag{23}$$

where, in hover OGE, $\overline{T}_h = \overline{T}_o$ is the factor giving the ratio of the thrust required to balance the gross weight plus the download (vertical drag D_v) to the gross weight, η_{oa} is the ratio of the rotor power to the engine power; i.e., the overall engine power utilization efficiency, c_{l_0}, as always, is the average blade-lift coefficient, assumed to exist at the $\overline{r} = 0.7$ blade section, c_{d_0} is the profile drag coefficient corresponding to the c_{l_0} value at Reynolds and Mach numbers at the $\overline{r} = 0.7$ blade station, $\Omega R = V_t$ is the tip speed in fps, I_0 is the induction coefficient determined from Fig. 3, w is the disc loading in psf, and σ_ρ is the relative air density corresponding to the ambient flight conditions.

The $\bar{T}_h$ factor in the most general case of fuselage plus wing and horizontal empennage submerged in the rotor downwash will be:

$$\bar{T}_h = 1 + (\Delta\bar{T}_f + \Delta\bar{T}_w + \Delta\bar{T}_{he}), \tag{24}$$

where the $\Delta\bar{T}$ values can be computed from Eqs. 20 and 21.

Using the single-rotor configuration as an encompassing example, the overall engine power utilization coefficient (η_{oa}) can be expressed (according to Eq. (2.20)[2]) as follows:

$$\eta_{oa} = 1 - \Delta\bar{P}_{tx} - \Delta\bar{P}_{cool} - \Delta\bar{P}_{tr}. \tag{25}$$

Here, $\Delta\bar{P}_{tx} = \Delta P_{tx}/SHP = 0.04$ to 0.07 is the relative power lost in the transmission, $\Delta\bar{P}_{cool} = \Delta P_{cool}/SHP =$ 0.01 to 0.02 is the relative power representing cooling losses in the turboshaft-type powerplant, and ΔP_{tr} is the relative power required for the tail rotor, which can be taken as

$$\Delta\bar{P}_{tr} = RP_{tr}/SHP \approx \eta_{oa}\chi_{tr}(RP_{tr}/RP). \tag{26}$$

The χ_{tr} coefficient in this equation expresses the influence of the main rotor on the tail rotor. It is indicated in the text preceding Eq. (2.21)[2] that when the tail-rotor blades facing the main rotor move from down to up, then $\chi_{tr} < 1.0$. When the direction of the tail-rotor rotation is reversed, this coefficient may be as high as 1.22. Consequently, this value must be separately determined for each of the helicopters selected for $(\widetilde{SHP}_h)_{req}$ determination.

The RP_{tr} quantity in Eq. (26) represents the rotor power required by the tail rotor to develop a thrust T_{tr} equal to the force required to balance the main-rotor torque times the $\bar{T}_{tr}$ coefficient, which can be expressed as

$$\bar{T}_{tr} = 1 + \Delta\bar{T}_{tr}, \tag{27}$$

where the additional relative thrust due to the "blocking effect" for the "pusher-type" tail rotor is (see Eq. (2.14)[2]):

$$\Delta\bar{T}_{tr} \approx 0.27\tilde{S}_{tr} \tag{28}$$

and for the pulling type

$$\Delta\bar{T}_{tr} \approx 0.76\tilde{S}_{tr}, \tag{29}$$

where $\tilde{S}_{tr} = S_{tr}/\pi R^2{}_{tr}$ is the ratio of the vertical tail area covered by the tail-rotor disc projection to the tail-rotor area.

Should the $RP_{tr} = f(T_{tr})$ relationship be known, then the RP_{tr} term in Eq. (26) can be found, once the tail-rotor thrust is computed as in Eq. (2.21)[2].

$$T_{tr} = RP(550/\Omega R)(\bar{T}_{tr}/\bar{l}_{tr}), \tag{30}$$

where $\bar{l}_{tr} = 1 + \bar{R}_{tr}$ is the relative distance between the main- and tail-rotor axes, and $\bar{R}_{tr} = R_{tr}/R$. The task of determining the $RP_{tr} = f(T_{tr})$ relationship can be accomplished through a subroutine based on the single-section approach, which is similar to that of finding $(\widetilde{SHP}_h)_{req}$ in hover OGE for the helicopter as a whole.

2.4.2 Specific Configurations

Single-Rotor Helicopter. The computational procedure for determination of $(\widetilde{SHP_h})_{req}$ for the single-rotor helicopter is based on Eq. (23). The highlights of that procedure are as follows.

Reynolds and Mach number values at $\bar{r} = 0.7$ blade station under specific ambient conditions are determined.

The main-rotor thrust-to-weight ratio $(\bar{T}_h)$ is estimated from Eq. (24) and the average blade-lift coefficients (c_{l_0}), assumed to be equal to c_{l_7} at the $\bar{r} = 0.7$ blade station, are computed from the following expression:

$$c_{l_0} = 6w\bar{T}_h/\rho_0\,\sigma_\rho\,\sigma(\Omega R)^2\chi \tag{31}$$

or, assuming that the tip-loss factor $\chi = 0.94$ and that $\rho_0 = 0.002378$ slugs/cu.ft,

$$c_{l_0} = 2684w\bar{T}_h/\sigma_\rho\,\sigma(\Omega R)^2. \tag{31a}$$

Next the representative profile drag coefficient corresponding to the previously computed c_{l_0} values are found from the $c_d = f(c_l)$ graphs at proper Re and M values. The induction coefficient (I_0) is determined from Fig. 3. Now the specific rotor power terms for profile and induced powers can be computed; the sum of which gives the total specific rotor power $(\widetilde{RP})$.

The tail-rotor contributions to the η_{oa} values start with determination (Eqs. (28) or (29)) of the total tail-rotor thrust increase factor, $\bar{T}_{tr}$. The total tail-rotor thrust required to compensate for main-rotor torque and overcome the "blocking effect" of the vertical fin can be obtained from Eq. (27), and the corresponding tail-rotor rotor power (RP_{tr}) can be obtained from the $RP_{tr} = f(T_{tr})$ graphs.

After establishing the χ_{tr} value, the η_{oa} estimate can be performed (assuming transmission $(\Delta\bar{P}_{tx})$ and cooling $(\Delta\bar{P}_{cool})$ losses) from the following relationship:

$$\chi_{oa} = (1 - \Delta\bar{P}_{tx} - \Delta\bar{P}_{cool})/[1 + \chi_{tr}(RP_{tr}/RP)]. \tag{32}$$

Coaxial Helicopter. The procedure outlined in Sect. 2.2 can be used for the determination of the $C_{Q_{co}}$ values for the isolated coaxial rotor with the following modifications.

The relative vertical drag $(\Delta\bar{T})$ is computed from Eq. (20) and the total download factor $\bar{T}_{h_{co}}$ is determined:

$$\bar{T}_{h_{co}} = 1 + \Delta\bar{T}_f + \Delta\bar{T}_w + \Delta\bar{T}_{he}, \tag{33}$$

which leads to the total thrust

$$T_{h_{co}} = \bar{T}_{h_{co}} W. \tag{34}$$

where W is the gross weight.

For the selected gross weights and ambient flight conditions (σ_ρ), the corresponding c_{l_0} values are computed from Eq. $(1.22)^2$ as

$$c_{l_0} = 6.4T_{h_{co}}/\pi R^2\rho_0\,\sigma_\rho\,(\Omega R)^2 k_T\sigma_{co}. \tag{35}$$

As always, the c_{d_0} corresponding to the above-determined c_{l_0} values are obtained from the c_l and c_d relationships at Reynolds and Mach numbers existing at the blade $\bar{r} = 0.7$ station.

Having the c_{l_0} and c_{d_0} values at given gross-weight levels, $C_{Q_{co}}$ is computed, and $(\widetilde{SHP_h})_{req}$ magnitudes in hp/lb can be obtained from the known $C_{Q_{co}}$ values as follows:

$$(\widetilde{SHP_h})_{req} = 4.32 \times 10^{-6} C_{Q_{co}} \sigma_p (\Omega R)^3 / w \eta_{oa}, \tag{36}$$

where (ΩR) is the rotor tip speed in fps, w is the disc loading in psf, and the overall transmission efficiency η_{oa} is determined from Eq. (25) where, obviously, the $\Delta \bar{P}_{tr}$ term is neglected.

2.4.3 *Comparison of Predictions With Flight Test Results*

The above-discussed simplified methods of predicting $(\widetilde{SHP_h})_{req}$ were compared with flight-test results for the single rotor as represented by the Boeing Vertol YUH-61A (Ref. 10) and Sikorsky UH-60A (Ref. 11), and for the coaxial as represented by the Sikorsky XH-59A ABC (Ref. 8). In all cases, three gross weights (one close to the design value, one higher, and one lower) were examined, leading to good agreements between predicted and experimental values. The relative percentile deviations of the predicted values from those obtained from actual flight tests shown in Fig. 13 indicates that those deviations were included within approximate limits of $+3\%$ to -4%. It appears, hence, that even the simplest approaches of Ref. 2 may be useful for predicting approximate shaft horsepower required in hover OGE by single-rotor and coaxial helicopters. [Note: Although not discussed in this paper, points for the tandem CH-47D are also shown in Fig. 13.]

However, It should be remembered that in performing the calculations, attention must be paid to such aspects as tip-loss-factor value should the $(\sqrt{C_T}/b)$ quantity become higher than 0.025.

3. Some Basic Aspects of Horizontal Flight Performance

With respect to forward flight, there are many areas where simplified approaches may be quite useful in facilitating sufficiently accurate predictions of the approximate performance of various helicopter configurations. Obviously, many such approaches have been discussed in Western literature as well as in Ref. 2. However, because of space and time limitations, only the simplest method of determining engine power required in horizontal flight along the lines of Ref. 2 will be discussed here.

3.1 Engine Power Required in Horizontal Flight

Often, it is more convenient to perform calculations of engine power required in horizontal flight under given ambient conditions by first calculating the so-called specific engine power; i.e., *SHP* required per pound of thrust or gross weight $(\widetilde{SHP_{hz}})_{req}$. In Western, as well as Soviet approaches, this calculation for helicopters of all configurations is usually expressed as follows:

$$(\widetilde{SHP_{hz}})_{req} = (\widetilde{RP_{pr}} + \widetilde{RP_{ind}} + \widetilde{RP_{pa}})/\eta_{oa_{hz}}, \tag{37}$$

where $\widetilde{RP_{pr}}$, $\widetilde{RP_{ind}}$, and $\widetilde{RP_{pa}}$ are profile induced and parasite specific rotor powers, respectively, while $\eta_{oa_{hz}}$ is the power utilization efficiency factor (overall transmission efficiency) in forward flight.

In the simplified approach of Ref. 2, all of the above terms can easily be estimated. For instance, the profile rotor power term $(\widetilde{RP_{pr}})$ can be directly determined from Figs. 14 and 15 (Figs. 4.6 and 4.7 of Ref. 2) once the C_T/σ value is computed, and angles of the thrust vector inclination (α_e) are roughly estimated.

The $\widetilde{RP}_{ind}$ term in Eq. (37) can be computed from Eq. (4.16)[2]; rewritten here as

$$\widetilde{RP}_{ind} = 0.257 w I_{\Sigma}/\sigma_{\rho} V, \tag{38}$$

where w is the main-rotor disc loading in psf, V is the speed of flight in knots, and σ_{ρ} is the air-density ratio corresponding to ambient conditions (pressure and temperature). The induction coefficient I_{Σ} accounts for all the induced power losses resulting from the nonuniformity of the downwash distribution of the isolated rotor(s), as well as mutual interaction of the rotors. For the single rotor, I_{Σ} is identical to I and can be directly obtained from Fig. 16 (Fig. 3.26[2]) at the given advance ratio $\mu \approx \overline{V}$ values. Once again, the corresponding tilt angle (α_{ϵ}) of the thrust vector should be roughly calculated. The tip-loss factor of 0.94 is already incorporated in the 0.257 coefficient in Eq. (38).

For both of the cases depicted in Figs. 14, 15, and 16, the approximate forward tilt of the thrust vector can be determined on the basis of the parasite drag of the nonlifting components as

$$\alpha_{\epsilon} \approx \arctan \frac{V^2 0.0034}{V^2 \hat{f} \sigma_{\rho}} \tag{39}$$

where flight speed V is in knots, $\hat{f}$ expresses the ratio of the equivalent flat-plate area (in sq.ft) of nonlifting helicopter components to the aircraft gross weight in lbs, and σ_{ρ} is the air density ratio.

With respect to multirotor (especially twin-rotor) configurations, the mutual interaction of the rotors is determined on the basis of the flat-wake concept, which will be discussed separately later.

The third term in Eq. (37), expressing the contribution of parasite drag of nonlifting helicopter components, is directly computed from Eq. (4.13)[2], written here as

$$\widetilde{RP}_{par} = 1.04 \times 10^{-5} V^3 \hat{f} \sigma_{\rho}, \tag{40}$$

where, as in Eq. (39), V is in knots and $\hat{f}$ is in square feet per pound.

In principle, the equivalent flat-plate area of nonlifting components per pound of helicopter gross weight must be estimated for each of the considered helicopters. However, in order to provide some feeling about the order of magnitude of this quantity, representative levels for $\hat{f}$ are shown in Fig. 17, based on Fig. 4.3 of Ref. 2.

The power utilization efficiency coefficient in forward flight $\eta_{oa_{hz}}$ can be estimated from Eq. (32) where, for the single-rotor configuration, the relative variation of tail-rotor to main-rotor power ratio with speed of flight must be assumed as, for instance, in Fig. 18, while the percentile transmission and cooling losses remain the same as in hover.

3.2 Flat-Wake Concept

3.2.1 General

The flat-wake concept, briefly discussed in Ref. 2, and very thoroughly investigated in Ref. 3, represents an interesting simplified approach toward determination of the induced velocity field generated by a rotor in horizontal flight. Although the stated validity of that concept is restricted to advance ratios enclosed within the following limits[2,3] (expressed in U.S. symbols):

$$1.63\sqrt{C_T} < \mu \leqslant 0.25,$$

it appears that it can be applied to $\mu > 0.25$ – even as high as $\mu = 0.4$. However, use of this concept at advance ratios below the stated lower limit may lead to erroneous results.

In the Soviet Union, it appears that practical applications of the flat-wake approach are widely used in interpreting and solving many problems of applied aerodynamics; for instance, main- and tail-rotor interference in single-rotor, and mutual-rotor interaction in multi-rotor, configurations.

In the latter respect, special graphs for estimating induced power of the side-by-side configuration at various lateral separations of the rotors and direction of rotation are contained in Ref. 2. Also included is a graph (which will be discussed later) for computing induced power of coaxials and tandems, as well as a procedure for combining the information from the coaxial and side-by-side graphs in dealing with the induced power problems of the quad- and tri-rotor configurations. Furthermore, the flat-wake concept is also used for the interpretation of the rotor-wing interaction in forward flight.

By contrast, in the West, it appears that except for the studies of Ormiston (Ref. 12), little attention has been focused on this concept. Consequently, at the present time, only Soviet data can be used. In view of this, it would be especially interesting to check the validity of the flat-wake scheme by comparing predicted induced velocities at various points in the rotor space with those actually measured.

3.2.2 Comparison of Flat-Wake Predicted and Measured Downwash Components

Fig. 19 (Fig. 4.28 of Ref. 5) shows the downwash velocity ($\bar{v}_y = f(\psi)$ at $\bar{r} = 0.7$) computed for a rotor with flat, untapered blades having $\sigma = 0.07$, and operating at $\alpha_d = 0^\circ$, $\mu = 0.15$, and $C_T = 0.0006$. The $\bar{v}_y(\psi)$ relationship represented by dashed lines was first computed for circulation constant with the azimuth and varying only with ($\bar{r}$) according to Eq. (4.91)[2]. Then, the variation of circulation with the azimuth (solid lines with crosses) was considered; assuming that $\Gamma = \Gamma_0 + \Gamma_1 \sin\psi + \Gamma_2 \cos 2\psi$. It can be seen from this figure that the assumption of $\tilde{\Gamma}(\psi) = \text{const}$ at $\bar{r} = 0.7$ has little influence on the $\bar{v}_y$ values, also computed at $\bar{r} = 0.7$. In both cases, a satisfactory agreement with test measurements is shown, although the $\bar{v}_y$ values computed on the $\Gamma(\psi) = \text{const}$ assumption appear to be even closer to the experimental results.

Another example for the validity of the flat-wake concept can be provided by Fig. 20 (also reproduced in Ref. 5 as Fig. 4.29). Here, the flat-wake predicted downwash relative values ($\bar{r} = -1.0$ to $\bar{r} = 1.0$) are compared at several azimuth positions; again showing relatively good agreement.

From the two examples (based on Soviet sources) of a comparison of rotor downwash velocity in forward flight as predicted by the flat-wake method with actual measurements, it appears that the flat-wake concept, in spite of its relative simplicity, can be a useful practical tool for predicting flow fields generated by a rotor in forward flight.

3.3 Aerodynamic Interaction of Twin-Rotor Configurations

3.3.1 General

Aerodynamic interaction of twin rotors, as developed by the flat-wake concept, is of special interest for the coaxial and tandem configurations since they permit one to determine the I_Σ factor in Eq. (38). For the coaxial (Eq. 3.35[2]):

$$I_{\Sigma_{co}} = I_{sr}(1 + \chi_{co}), \tag{41}$$

where I_{sr}, obtained from Fig. 16 ($I_{sr} = I$), is the induction factor for the single rotor, and χ_{co} expresses the ratio of the induced velocity averaged over the disc of the upper rotor generated by the lower rotor to the induced velocity of the lower rotor, also averaged over the disc. It can be anticipated that the inductive influence of the lower rotor on the upper one would strongly depend on their relative separation ($\bar{y}_1 = y_1/R$). This is clearly evident from Fig. 21 (corresponding to Fig. 3.28[2]), where $\chi_{co} = f(\bar{y}_1)$ is shown.

Similar to the coaxial, the tandem vertical separation of the rotors; namely, relative elevation of the rear rotor over the front rotor, is the most important parameter. Furthermore, according to Ref. 2, the graph shown in Fig. 21 can be used for determination of the $I_{\Sigma_{tan}}$ factor in Eq.(38). This time, the induced power factor is expressed as

$$I_{\Sigma_{tan}} = (I_{sr} + \Delta I_{tan}). \tag{42}$$

where, as before, I_{sr} is the induction factor for the single rotor obtained from Fig. 16 (I_{sr} = I).

3.3.2 Actual Comparisons

Coaxial. Because full-scale test data for coaxial rotors could not be located, results of wind-tunnel investigations of a small model (Refs. 13 and 14) were used. In Fig. 12 of Ref. 14, the C_T/σ vs. C_Q/σ relationships are shown at $\mu = 0.16$ with a rotor disc angle of 0°, while relative separation of the rotors was $\bar{y}_1$ = 0, 0.21, 0.42, and 0.63. Using numerical inputs represented by the test points, ratios of induced power of rotors with the non-zero separations to that of the rotor with zero gap (four-bladed rotor) were calculated, assuming as in Ref. 13 that the blade $c_{d_{min}} = 0.0148$ (open symbols in Fig. 22). In order to investigate the sensitivity of the results to the estimated profile power levels, a lower minimum blade profile drag value of 0.0128 (instead of 0.0148) was assumed, and the induced power ratios were recalculated and marked as closed symbols in Fig. 22. The experimentally obtained induced power ratios were then compared with those based on Fig. 21. Finally, the curve of $RP_{ind_{\bar{y}}}/RP_{ind_{\bar{y}=0}}$, shown in Fig. 22 was computed from the following relationship:

$$RP_{ind_{\bar{y}_1}}/RP_{ind_{\bar{y}_{1=0}}} = (1 + \chi_{co})/2, \tag{43}$$

where χ_{co} was read from Fig. 21, and the denominator "2" corresponds to the zero-gap case.

A curve showing the induced power ratios established through a simple momentum approach — assuming an increase in the cross-section area of the slipstream due to rotor separation — is also shown in Fig. 22.

Comparing the curve based on Ref. 2 with test-derived points resulting from the assumption that the blade $c_{d_{0_{min}}} = 0.0148$, one would see that although the trend indicated by both approaches is similar, there are noticeable differences in the predicted induced power ratios.

An assumption of $c_{d_{min}} = 0.0128$ (closed symbols in Fig. 22) indicates that the points corresponding to $C_T/\sigma = 0.04$ and $\bar{y}_1 < 0.42$ would now come quite close to the curve based on Ref. 2. However, the point corresponding to $\bar{y}_1 = 0.63$ and all points related to $C_T/\sigma = 0.06$ would still suggest that relative reductions in induced power of the coaxials with respect to the zero-gap configuration would be about 10 to 12% better than predicted by Ref. 2.

In view of these discrepancies and sensitivity of the results to the blade profile-drag assumption, an additional verification of Fig. 21 regarding the induced power aspects of coaxial rotors in horizontal translation appears appropriate.

While not discussed in detail in this paper, it is interesting to note that results of Boeing-Vertol model wind-tunnel tests indicated that the approach based on Ref. 2, and reflected in Fig. 21, tends to under-predict the induced power coefficients in forward flight of tandems by a relative deviation ranging from about 7 percent at small rear-rotor elevations ($\bar{y}_1 \approx 0.1$), to about 3 percent when $\bar{y}_1 \approx 0.75$.

3.4 Tests vs. Predicted SHP Required in Horizontal Flight

3.4.1 UH-60A SHP Required

Engine power required in horizontal flight at a gross weight of 15,000 lb and a density altitude of 2060 ft ($\sigma_\rho \approx 0.94$) was selected for comparison.

The equivalent flat-plate area for parasite drag of nonlifting components was estimated as $f = 27$ sq.ft. This corresponds to $\hat{f} = 1.66 \times 10^{-3}$ at the primary mission gross weight of 16,200 lb. It can be seen from Fig. 17 that these $\hat{f}$ values are close to those given by curve 3, corresponding to contemporary helicopters.

The estimated engine power required was plotted in Fig. 23. Looking at this figure, one will note that in the considered case, engine power-required predictions based on the simplified approach of Ref. 2 are very good, with the exception of the high-speed point at 161.9 knots.

3.4.2 Relative Deviations in SHP Required for the UH-60A and CH-47D Helicopters

Relative deviations between the computed and test-determined SHP_{req} for the UH-60A are plotted in Fig. 24, where relative deviations in SHP_{req} are also shown for the tandem helicopter (CH-47D at 33,000-lb gross weight). As in the single-rotor case, the highest deviations, which are underestimates in both cases, appear in the V_{max} region. This may be due in part to the fact that in the simplest approach of Ref. 2 used in the computation, constant values of the equivalent flat-plate areas were assumed where, in fact, they may increase at high speeds due to the varying attitude of the fuselage.

4. *Concluding Remarks*

Approximate simplified methods for helicopter performance predictions that can be applied with confidence to such engineering tasks as concept formulation and preliminary design are, in principle, available in both the West and the Soviet Union. However, in the West, they are mostly remnants of past efforts in the fifties and sixties and, although their accuracy is quite good[1], there is little effort to either update them, or develop new ones. By contrast, it appears that in the Soviet school, there have been more recent efforts to systematically develop simplified, but sufficiently accurate, approaches to rotary-wing performance predictions and present them under the form of simple analytical expressions and auxiliary graphs; thus making them well suited to many practical tasks of rotary-wing design.

Vil'dgrube's book[2], which exemplifies that trend in the Soviet Union, was examined and a number of the simple methods and procedures presented were selected and reconstructed, using U.S. symbols and measurement units, making it easier for the Western reader to follow and apply them. These methods were also used in comparing predicted values with the results of mainly full-scale tests of Western products. Examples of such comparisons were given in the following areas.

Single and Coaxial Configurations in Hover, OGE

1. Predictions of isolated rotor characteristics.
2. Determination of download of complete helicopters.
3. Predictions of engine power required.

Horizontal Flight

1. Determination of engine power required in horizontal flight for single-rotor helicopters.

On the basis of comparisons of predicted values with tower and flight test results of Western helicopters, it appears that in the field directly related to performance predictions of single-rotors and coaxials in hover, and the single-rotor horizontal flight, the simple methods and procedures based on Vil'dgrube's approaches produce results that are in good, or even often very good, agreement with experimental results. Consequently, they may be recommended for such practical engineering applications as concept formulation and preliminary design of helicopters.

Extensive use of graphs is made in the Soviet simplified approaches. This appears to be in sharp contrast to current Western practice where, with ever-increasing reliance on computer programs, techniques of 'earlier days' of prescribing necessary inputs under the form of work graphs has almost disappeared[1].

It should be noted, however, that some graphs from Ref. 2 should be applied with caution, particularly to such cases as determination of specific rotor profile ($\widetilde{RP}_{pr}$) in horizontal flight, or estimation of the induction coefficient (I_0) for isolated rotors in the same regime of flight. In both cases, various assumptions were made when the graphs were developed. Should, in actual cases of determining isolated rotor characteristics or helicopter performance, the rotor parameters and operational conditions be radically different from the specified ones, suitable corrections to the values obtained from the graphs should be applied.

Among the various simplified approaches of Ref. 2, perhaps the flat-wake concept, which in the Soviet school is useful in explaining and providing approximate relationships for many aerodynamic phenomenon of horizontal flight, should attract more attention in the West.

In general, one may state that, of course, it would be foolish to turn the clock back and forego all the opportunities offered by constantly advancing computerized techniques to develop potentially more and more precise ways of treating all aerodynamic phenomenon of rotary-wing aircraft. Nonetheless, it appears that it would still be desirable to continually devote some effort in the West to formulate accurate, but at the same time, as simple as possible approximate relationships that could be applied with confidence to many areas of engineering aerodynamics. As a guide to determine the areas of application and degree of sophistication, we wish to repeat after Gessow[1] a saying of Albert Einstein: "Things should be done as simply as possible, but not simpler."

References

1. Gessow, A. "Nikolsky Honorary Lecture: Understanding and Predicting Helicopter Behavior – Then and Now," Journal of the Americal Helicopter Society, Vol. 31, No. 1, Jan 1986, pp 3-28.

2. Vil'dgrube, L.S. "Vertolety, Raschet Integral'nykh Aerodynamicheskikh Kharakteristick i Letno-Mekhanicheskikh Danykh" (Helicopters – Calculations of Integral Aerodynamic Characteristics and Flight-Mechanics Data). Moscow, "Mashinostroyeniye," 1977.

3. Baskin, V.E., L.S. Vil'dgrube, Ye S. Vozhdayev, and G.I. Maykapar. "Theory of the Lifting Airscrew," NASA TT F-823, Feb. 1976.

4. Gessow, A. and Meyers, G.D., Jr. "Aerodynamics of Helicopters." MacMillan, 1952.

5. Stepniewski, W.Z. and C.N. Keyes. "Rotary-Wing Aerodynamics." Dover Publications, Inc., 1984.

6. Rosenstein, H. "Whirl Tower Investigation of the UH-61A Elliptical Tip Main Rotor." Boeing Vertol Co. Internal Report D210-1128-1, Sep 1976.

7. Harrington, R.D. "Full-Scale Tunnel Investigation of the Static Thrust Performance of a Coaxial Helicopter Rotor." NACA TN-2318, 1951.

8. Arents, D.N. "An Assessment of the Hover Performance of the XH-59A Advanced Blade Concept Demonstration Helicopter." USAAMRDL-TN-25, May 1977.

9. Acree, C.W., Jr. "Results of the First Complete Static Calibration of the RSRA Rotor-Load-Measurement System." NASA TP-2327, Aug 1984.

10. Winn, L.A., et al. "Government Competitive Tests Utility Tactical Transport Aircraft System (UTTAS) – Boeing Vertol YUH-61A Helicopter." Final Report AD-B-031-0854, Nov 1976.

11. Negata, J.I., et al. "Airworthiness and Flight Characteristics Evaluation UH-60A (Black Hawk) Helicopter." U.S. Army AVRADCOM, USAAEFA Project 77-17, Sep 1981.

12. Ormiston, Robert A. "An Actuator Disc Theory for Rotor Wake Induced Velocities." AGARD-CCP 111, Sep 1972.

13. Azuma, Akira, et al. "Application of the Local Momentum Theory to the Aerodynamic Characteristics of Multi-Rotor Systems." Vertica Vol. 3, No. 2, pp. 131-144, 1979.

14. Saito, S. and A. Azuma. "A Numerical Approach to Co-Axial Rotor Aerodynamics." Vertica Vol. 8, pp. 253-266, 1982.

Acknowledgements

The authors wish to express their sincere thanks for the contributions of the following individuals and companies: First, technical support and assistance was provided by John M. Davis (U.S. Army) and Dr. George Matthews (University of Virginia). James S. Hayden (U.S. Army) was instrumental in obtaining some flight test results. With respect to industry, it should be mentioned that Boeing Vertol and Sikorsky companies supplied valuable information regarding their products and test results. As for individual contributions, Messrs. Charles N. Keys and Leon Dadone of Boeing Vertol should be cited for their help in obtaining the necessary data and technical contributions. Finally, the authors are grateful for the assistance of Mrs. Wanda L. Metz in setting up the text and for many helpful suggestions.

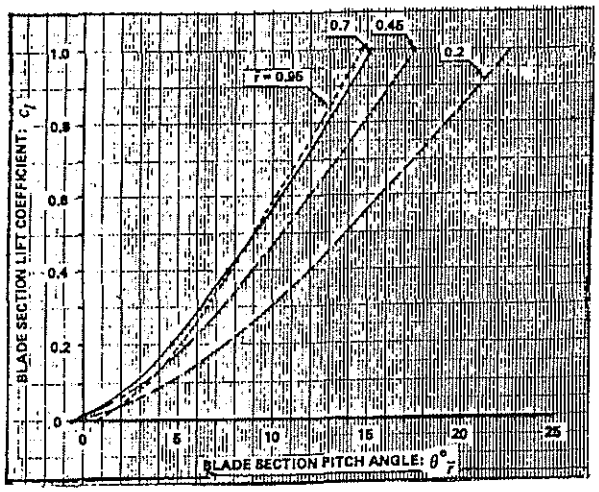

Figure 1. Blade-section lift coefficient vs. blade-section pitch angle for the YUH-61A rotor

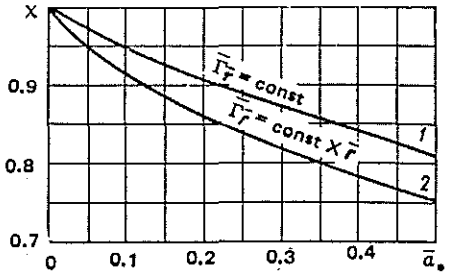

Figure 2. Graph for estimating tip-loss factor

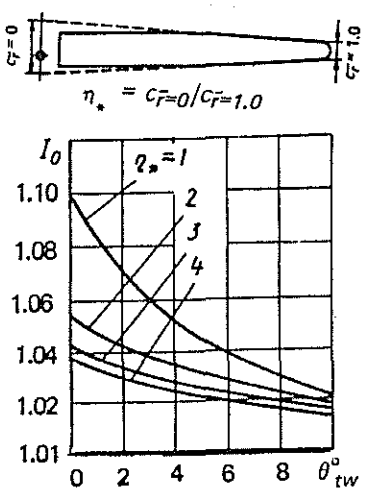

Figure 3. Induction coefficient vs. blade linear twist for various taper ratio values

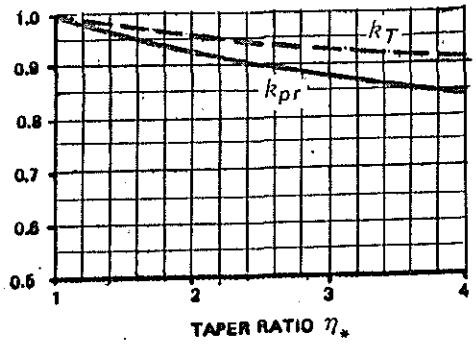

Figure 4. Coefficients k_T and k_{pr} vs. blade taper ratio

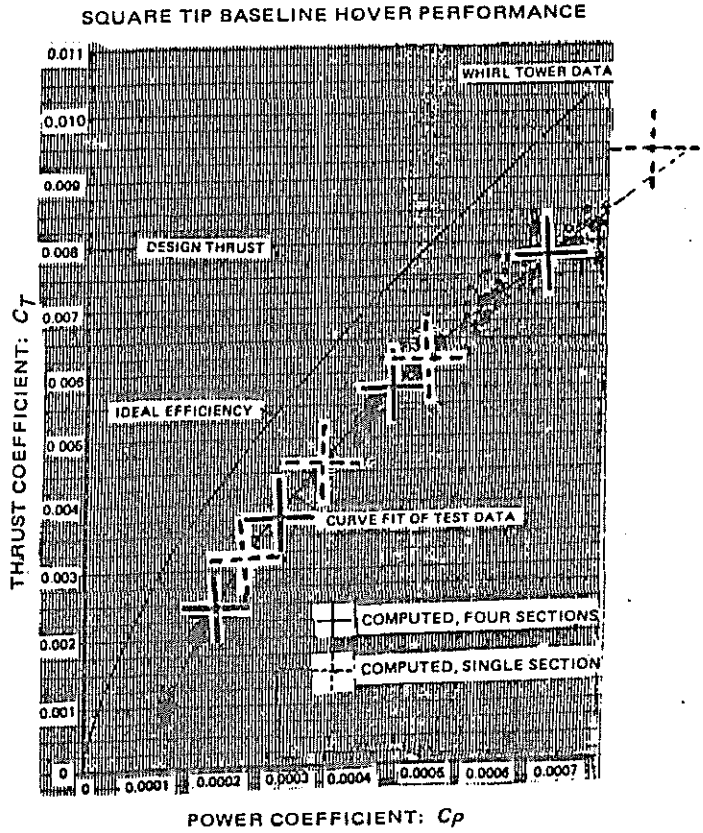

Figure 5. Experimental and computed hover performance for a full-scale YUH-61A rotor

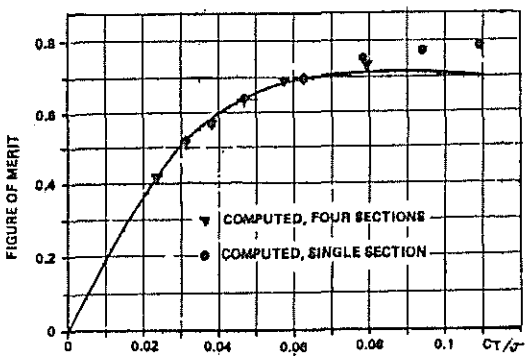

Figure 6. Computed figure-of-merit values vs. full-scale tests for the YUH-61A rotor in hover OGE

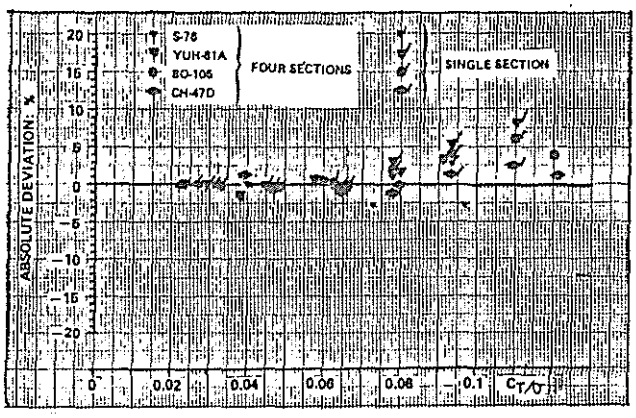

Figure 7. Summary plot of absolute percentile deviations of calculated FM values from those derived from tests

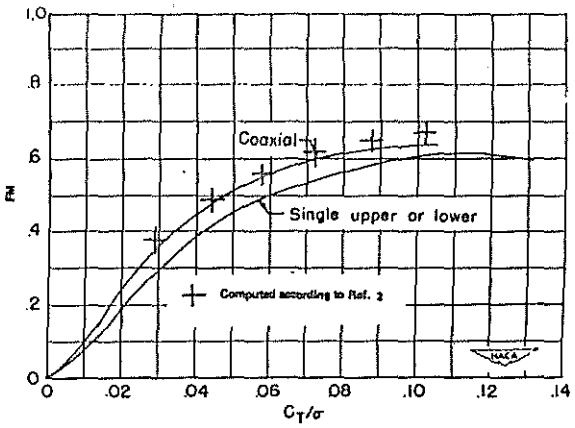

Figure 9. Variation of FM and C_T/σ for a coaxial rotor with tapered blades: $\eta_* = 2.92$

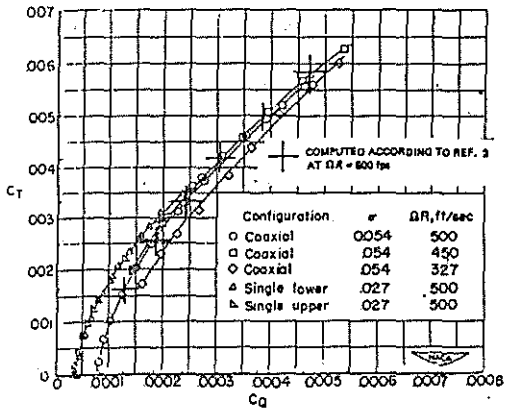

Figure 8. Variation of C_T and C_Q for a coaxial rotor with tapered blades: $\eta_* = 2.92$

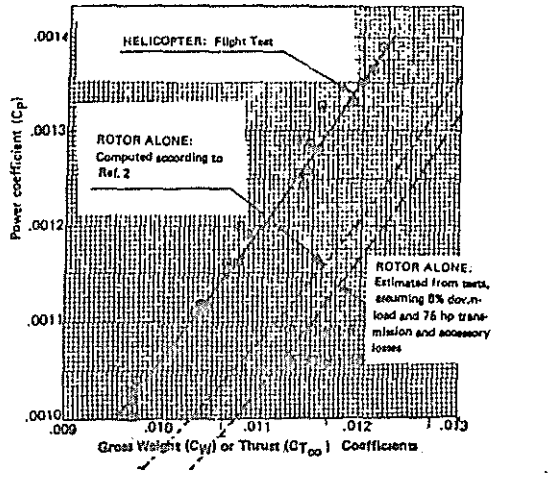

Figure 10. XH-59A Out-of-ground effect hover performance

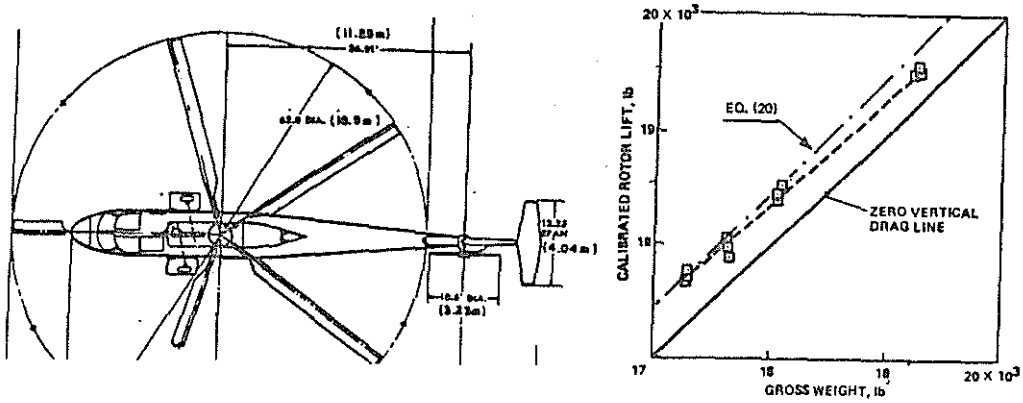

Figure 11. Load-cell system lift measurement vs. corrected gross weight for hover OGE

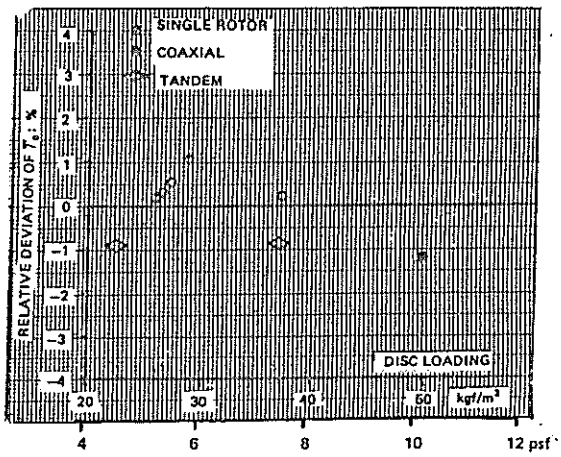

Figure 12. Relative deviations of thrust to gross-weight ratio in hover OGE

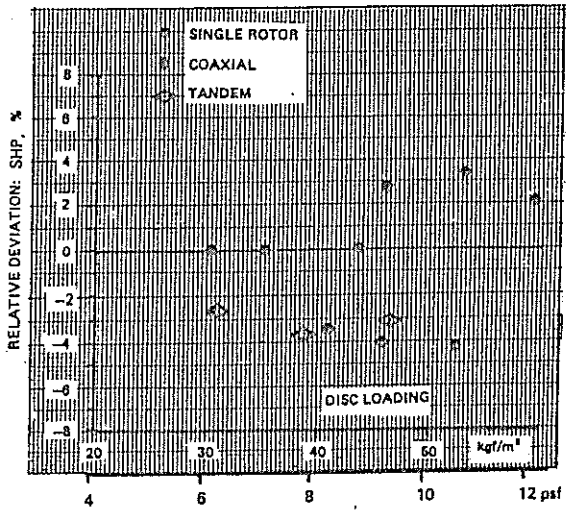

Figure 13. Summary chart of relative deviations computed from test-established engine power in hover OGE

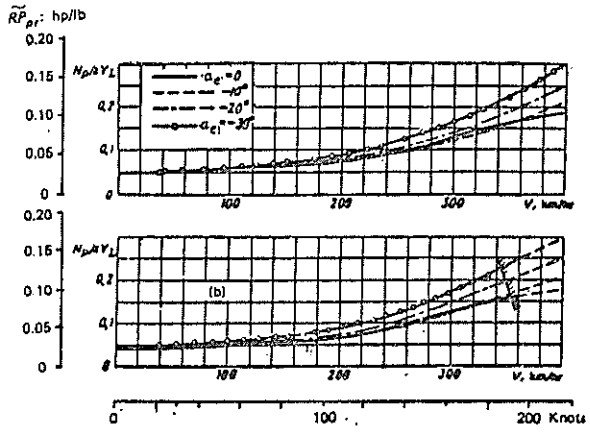

Figure 14. Determination of $\widetilde{RP}_{pr}$ at ΩR = 720 fps, where (a) corresponds to C_T/σ = 0.06 and (b) corresponds to C_T/σ = 0.07. Hatched lines indicate incipience of blade stall.

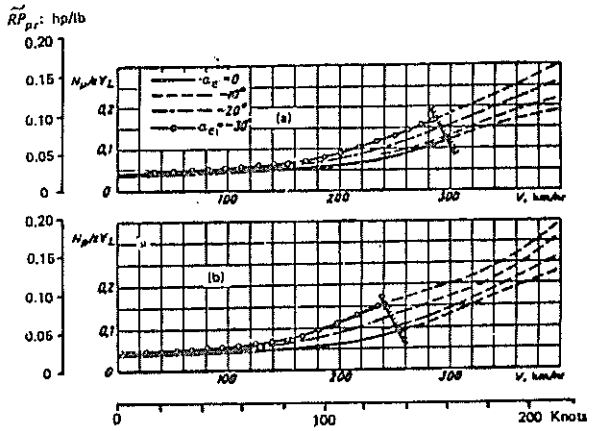

Figure 15. Determination of $\widetilde{RP}_{pr}$ at ΩR = 720 fps, where (a) corresponds to C_T/σ = 0.08, and (b) corresponds to C_T/σ = 0.09. Hatched lines indicate incipience of blade stall.

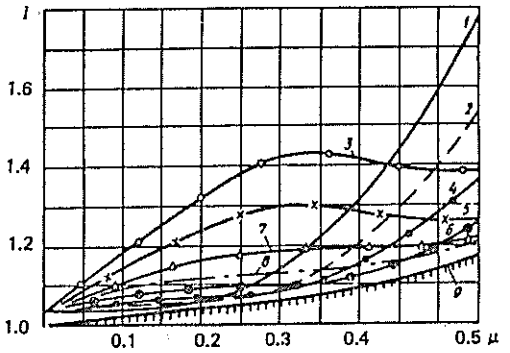

Figure 16. Graph for determining I for rectangular blades with a small taper at the tip and $\theta_{tw} = -7°$. Curve 1 signifies α_e @ 5°, 2 @ 0°, 3 @ 30°, 4 @ −5°, 5 @ −25°, 6 @ −10°, 7 @ −20°, 8 @ −15°, and 9 = I_{min}. $I = I_\Sigma \approx$ const at $0.07 \leqslant \sigma \leqslant 0.13$, and $0.065 \leqslant C_T/\sigma \leqslant 0.11$.

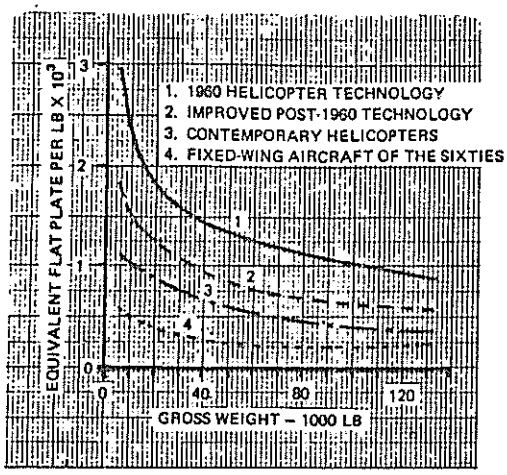

Figure 17. Equivalent flat-plate area of nonlifting components per pound of gross weight

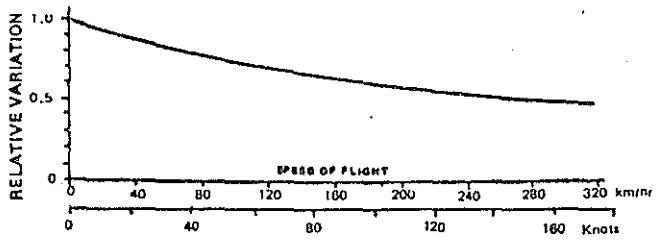

Figure 18. Relative variation of the tail-rotor to the main-rotor ratio

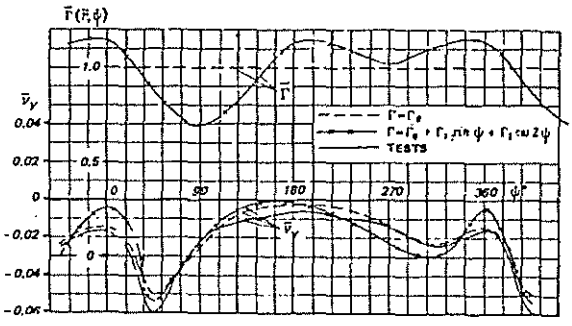

Figure 19. Comparison of predicted and measured $\bar{v}_y = f(\psi)$ at $\bar{r} = 0.7$

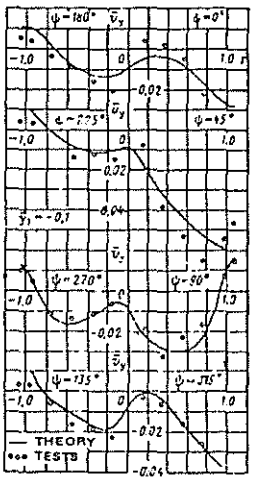

Figure 20. Predictions compared with tests of $\bar{v}_y(\bar{r})$ at several azimuth angles

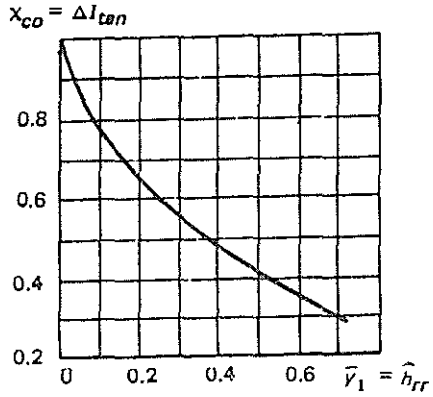

Figure 21. Graph for determining I_Σ for coaxials and tandems

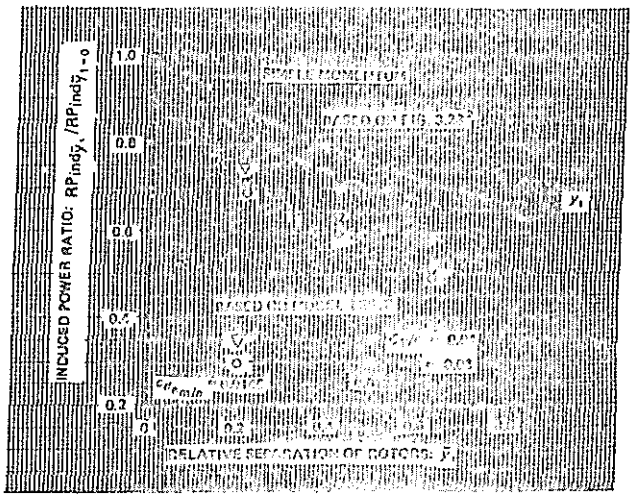

Figure 22. Forward flight induced power ratio of coaxial rotors having various rotor separations to that of a rotor with zero gap

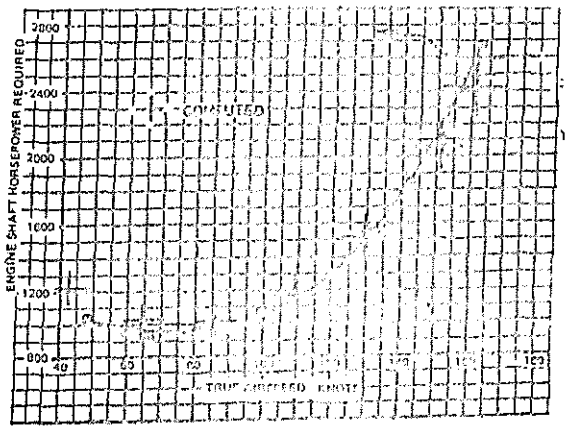

Figure 23. Comparison of computed and test-flight-established engine power required vs. speed for UH-60A helicopter

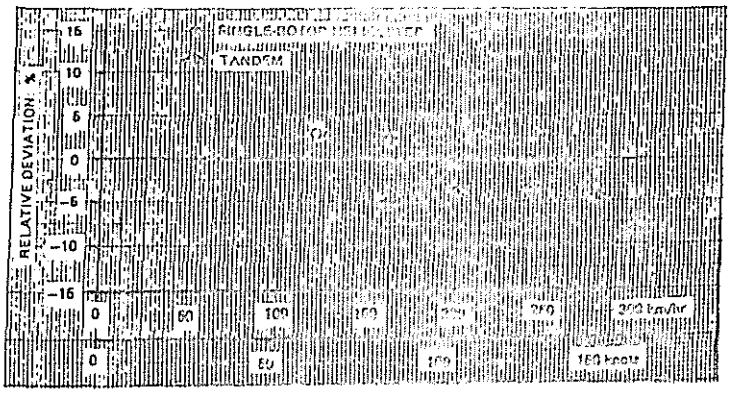

Figure 24. Relative deviations of SHP required in horizontal flight as computed by the methods of Ref. 2 from that established by flight tests